Dynamic Stokes shift in green fluorescent protein variants

Paul Abbyad, William Childs, Xinghua Shi, and Steven G. Boxer*

Department of Chemistry, Stanford University, Stanford, CA 94305-5080

Edited by Ahmed H. Zewail, California Institute of Technology, Pasadena, CA, and approved October 29, 2007 (received for review July 1, 2007)

Solvent reorganization around the excited state of a chromophore leads to an emission shift to longer wavelengths during the excited-state lifetime. This solvation response is absent in wild-type green fluorescent protein, and this has been attributed to rigidity in the chromophore's environment necessary to exclude nonradiative transitions to the ground state. The fluorescent protein mPlum was developed via directed evolution by selection for red emission, and we use time-resolved fluorescence to study the dynamic Stokes shift through its evolutionary history. The far-red emission of mPlum is attributed to a picosecond solvation response that is observed at all temperatures above the glass transition. This time-dependent shift in emission is not observed in its evolutionary ancestors, suggesting that selective pressure has produced a chromophore environment that allows solvent reorganization. The evolutionary pathway and structures of related fluorescent proteins suggest the role of a single residue in close proximity to the chromophore as the primary cause of the solvation response.

GFP | solvation response | ultrafast

The Stokes shift between the absorption and emission of a chromophore reflects the displacement in potential surface between the ground and excited states and loss of vibrational energy in the excited state. For chromophores that have a large increase in dipole moment between the ground and excited state, the fluorescence emission maximum often depends strongly on solvent polarity in simple fluid solvents and the emission is observed to shift to longer wavelengths during the excited-state lifetime. Such dynamic Stokes shifts have been extensively studied as a probe of solvent polarity and dynamics (1–3). For a chromophore in a protein, the solvent is much more organized and constrained than in a simple solvent, so the capacity for solvation is expected to be quite different, yet important for function, from that in a simple solvent. There are relatively few studies of dynamic Stokes shifts in proteins: a few dye–protein complexes (4–7), antibodies bound to fluorescein (8), surface tryptophan residues as a probe of hydration (9–11), unnatural amino acids (12, 13), studies on cytochrome *c* (14, 15), and photosynthetic antenna complexes (16). In contrast to small-molecule solvents, it should in principle be possible to dissect the contributions of individual amino acids to the solvation response of a protein and even its evolutionary history, although such an analysis has not to our knowledge been reported.

GFPs would seem to be ideal candidates for measurements of the dynamic Stokes shift because the chromophore is intrinsic to the protein and structurally well characterized (17), and the 6- to 7-debye change in dipole moment upon excitation of the chromophore (18) is as large as for most dyes used to probe solvation dynamics in simple fluid solvents. Furthermore, recent studies confirmed that, like conventional solvation probes, the emission of synthetic GFP chromophores shifts substantially as a function of solvent polarity (19). Despite these properties, the Stokes shifts in most GFPs are small, suggesting that the environment in the region around the chromophore is quite rigid. Both the synthetic GFP chromophore (20) and the chromophore in denatured protein (21) exhibit a very low fluorescence quantum yield, likely because the chromophore undergoes isomerization and nonfluorescent relaxation when the solvent is flexible. Consistent with this theory, the isolated chromophore fluorescence quantum yield increases dramatically if the solvent is frozen (22), and low temperature and/or high pressure can increase the quantum yield for GFP variants with intrinsically low quantum yields, such as blue fluorescent protein (23). Thus, a high fluorescence quantum yield, which is desirable for native function (and biotechnology), and the conditions of protein flexibility needed to observe a dynamic Stokes shift appear to be mutually exclusive for GFP variants.

Recently, Wang *et al.* (24) reported a very red-emitting fluorescent protein named mPlum that was created by a directed evolution strategy. mPlum is derived from DsRed, which was isolated from *Discosoma* coral. DsRed displays bright, red fluorescence, but it is a strongly associated tetramer, so its use as a genetic marker is limited. Through a combination of rational design and stepwise random mutagenesis, Tsien and colleagues (10) generated a monomeric version of DsRed known as monomeric red fluorescent protein (mRFP). Wang *et al.* then used somatic hypermutation to generate a huge and diverse library of mRFP mutants, which were screened for brightness and the reddest possible emission maximum by using a FACS; the reddest populations were subjected to further rounds of directed evolution. In this selection process, the FACS excitation wavelength was fixed at 568 nm, so the selection was not just for a red emitter but also for a large Stokes shift. Interestingly, both mRFP and mPlum absorb maximally at ≈588 nm, but they emit at 607 and 649 nm, respectively. Thus, mPlum has a much larger Stokes shift than is typical for GFPs, and here we investigate the nature of this Stokes shift.

Results

The absorption spectra of the isolated and purified mPlum and immature mPlum are shown in Fig. 1. The extra conjugated double bond of the mature form of chromophore leads to the large red shift in the spectrum relative to the immature form. An excitation spectrum of the mature protein confirmed that the minor peaks at 375 and 345 nm in the absorption spectrum of the mature form (Fig. 1*C*) are the higher energy states of the mature form and not contamination from the immature form. Isolating the mature form was important to ensure that the spectroscopic and crystallographic data were of a pure protein and not a mixture of the mature and immature forms. The structures of the chromophores for mature and immature mPlum are shown in Fig. 1 *B* and *D* (S. J. Remington and X. Shu, personal communication). The extension of the chromophore is confirmed in the crystal structure by a change in the hybridization state of the

Author contributions: P.A., W.C., X.S., and S.G.B. designed research; and P.A., W.C., and X.S. performed research.

The authors declare no conflict of interest.

This article is a PNAS Direct Submission.

*To whom correspondence should be addressed at: Stanford University, Keck Science Building, 380 Roth Way, Stanford, CA 94305. E-mail: sboxer@stanford.edu.

This article contains supporting information online at www.pnas.org/cgi/content/full/0706185104/DC1.

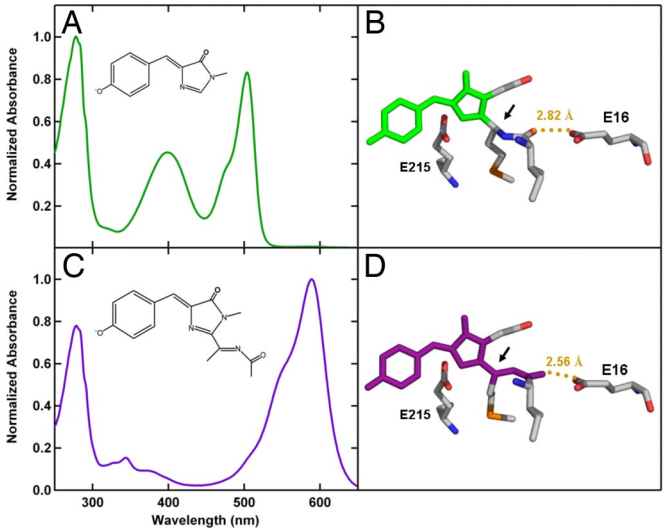

Fig. 1. Chromophore characterization. (*A*) Absorption spectra of isolated immature mPlum with corresponding chromophore chemical structure. (*B*) Crystal structure of immature mPlum chromophore including neighboring residues E16 and E215 (S. J. Remington and X. Shu, personal communication). The arrow points to the sp^3 hybridized carbon of immature mPlum. The dotted line indicates the hydrogen bond between the glutamic acid and carbonyl of residue 65. (*C*) Same as *A* for mature mPlum. (*D*) Same as *B* for mature mPlum. The arrow points to the sp^2 hybridized carbon of mature mPlum.

exocyclic carbon (indicated by an arrow in Fig. 1) from sp^3 to sp^2. Neighboring residues to the chromophore, E16 and E215, also are shown.

Fig. 2 shows the fluorescence excitation and emission spectra of mRFP, mRaspberry, and mPlum at pH 7 and pH 11. The pK_a of the mPlum chromophore is <4.5 (25); therefore, the chromophore is almost exclusively in the anionic form at all pH values described here. mRFP has an excitation maximum at 588 nm and an emission maximum at 612 nm. mRaspberry is an intermediate in the evolution process from mRFP to mPlum and has excitation and emission maxima of 596 and 624 nm, respectively. The mPlum spectra are characterized by an excitation maximum at 588 nm and an emission maximum at 649 nm in pH 7 buffer. At higher pH, the excitation shifts to the blue and the emission shifts

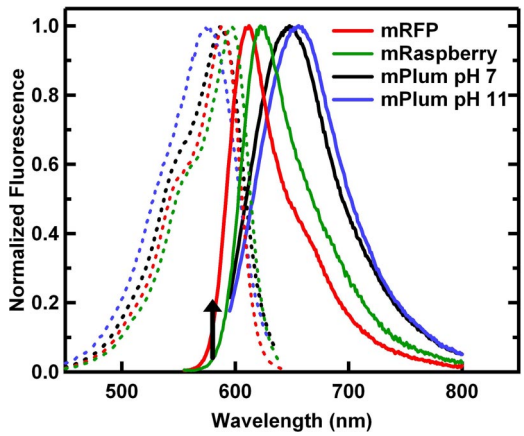

Fig. 2. Steady-state fluorescence spectra. Normalized steady-state excitation (dotted line) and fluorescence spectra (solid line) of mRFP at pH 7 (red), mRaspberry at pH 7 (green), and mPlum at pH 7 (black) and pH 11 (blue). The excitation wavelength for the emission spectrum and time-resolved experiments of mPlum is 580 nm (540 nm for mRFP and mRaspberry) and is indicated by an arrow. All excitation spectra were obtained at a wavelength of 650 nm.

to the red, so that in pH 11 buffer, the Stokes shift is 21 nm larger with peak wavelengths of 576 nm and 658 nm for excitation and emission, respectively. Treating the pH dependence as a titration, the apparent pK_a of the titratable group in mPlum is 10.7. Similar pH-dependent shifts in the excitation peak were observed for other proteins evolved from mRFP, such as mCherry (apparent pK_a of 10.29) and mStrawberry (apparent pK_a of 9.75) (26); however, for these proteins, the emission shift is to the blue rather than to the red, as observed for mPlum. The fluorescence quantum yield of mPlum is 0.10, substantially lower than mRFP, which is 0.26 (24).

Fluorescence decays were obtained by upconversion spectroscopy and time-correlated single photon counting (TCSPC) at 10 discrete energies from 13,946 cm^{-1} (717.0 nm) to 16,946 cm^{-1} (617.4 nm) in 250-cm^{-1} increments. Fig. 3*A* shows the 627- and 692-nm fluorescence decays obtained by fluorescence upconversion spectroscopy for mPlum. The decays were well fitted by the sum of two exponentials convoluted with the instrument response. The 627-nm trace is characterized by a fast decay of 39 ps that makes up 28% of the total amplitude followed by a slower decay of 573 ps. The kinetics at redder wavelengths show a fast rise with a lifetime of 39 ps and a −27% amplitude contribution followed by a slower decay of 723 ps. The decay could not be fitted well with either a sum of exponentials or a stretched exponential without a negative amplitude contribution. The negative amplitude contribution is consistent with an increase in the excited-state population at this wavelength, the hallmark of a dynamic Stokes shift associated with the solvation of excited chromophores. mPlum's evolutionary ancestors, mRFP and mRaspberry, do not show a similar solvation response. In the case of mRFP, the fluorescence decays show no rise, and decays at both red and blue wavelengths are well described by a single exponential decay. For mRaspberry, there may be a rise at red wavelengths, but it is very small compared with mPlum with a total amplitude of <4%.

Fig. 3*B* shows normalized, time-resolved fluorescence spectra. The spectra are fit to log-normal line shapes and show a fast shift in time to lower energy. Peak fluorescence energy versus time for samples in pH 7 and pH 11 buffers are shown in Fig. 3*C*. The dynamic Stokes shift at pH 7 is characterized by a fast shift that is largely completed by 500 ps. It can be fitted to a double exponential with amplitudes of 301 and 492 cm^{-1} and lifetimes of 4.3 and 71 ps, respectively. At pH 11, a similar fast component is observed with amplitudes of 268 and 357 cm^{-1} and lifetimes of 3.3 and 50 ps, respectively. In pH 11 buffer, the dynamic Stokes shift also exhibits a longer time component, with an amplitude of 175 cm^{-1} and a lifetime of 900 ps. Note that uncertainty in the emission maximum is greater at early time due to the lack of data points on the high-energy side. The lack of data points is due to light contamination from upconverted scattered excitation light. See supporting information (SI) *Text* for a detailed description of the data analysis. Dynamic Stokes shifts for mPlum, mRaspberry, and mRFP at pH 7 from TCSPC are shown in Fig. 3*D*. Both mRaspberry and mRFP show a negligible shift in peak emission wavelength. Upconversion experiments confirmed that there is also not a significant shift on faster timescales.

The effect of temperature on the steady-state fluorescence emission spectrum of mPlum was studied from 298 to 140 K in pH 7 buffer (Fig. 4*A*). As the temperature was lowered, the steady-state emission maximum decreased from 648 nm (15,432 cm^{-1}) at 298 K to 624 nm (16,026 cm^{-1}) at 140 K. The glass transition temperature for the 60/40 glycerol/buffer solution is ≈200 K. There is a steady shift in emission maximum above the glass transition; however, below the glass transition, there is only a small dependence of the emission maximum upon a further decrease in temperature. The peak of the excitation spectrum also shifts to lower wavelength with decreasing temperature, from 588 nm (17,007 cm^{-1}) at 298 K to 582 nm (17,182 cm^{-1})

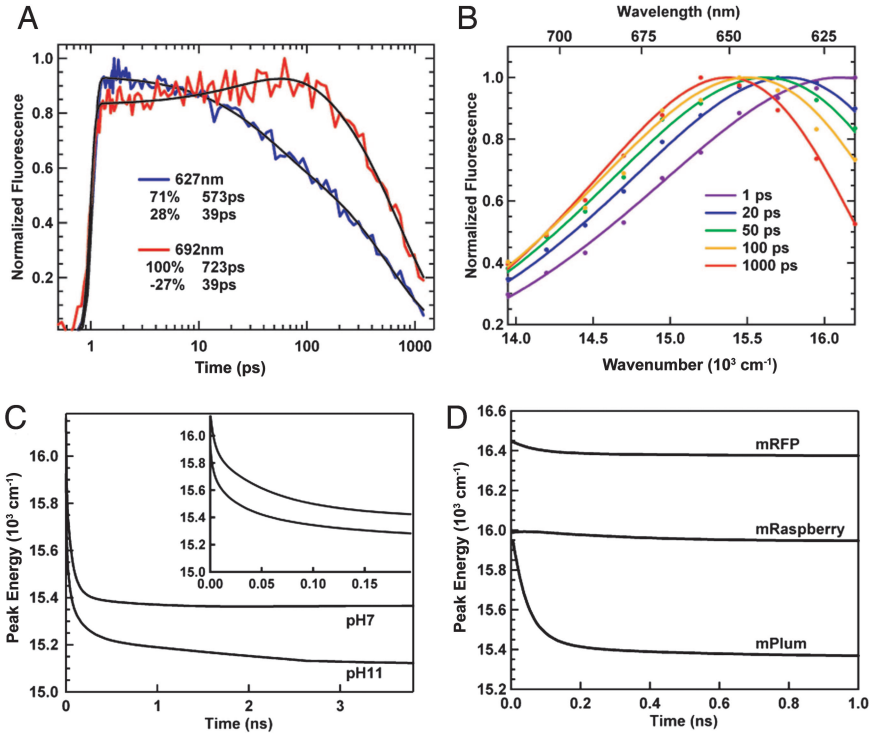

Fig. 3. Time-resolved measurements. (*A*) Normalized time-resolved fluorescence decays for mPlum, pH 7, at 627 nm (blue) and 692 nm (red) as obtained by upconversion spectroscopy with excitation at 580 nm. Excitation occurs at 1 ps on the time axis. (*B*) Reconstructed time-resolved fluorescence spectra obtained at 1, 20, 50, 100, and 1,000 ps as obtained by upconversion spectroscopy and TCSPC. The solid lines are log normal line-shape fits to the data. (*C*) Fluorescence emission maximum as a function of time for mPlum at pH 7 and pH 11 as obtained from upconversion spectroscopy and TCSPC as described in the text. (*Inset*) Detail for the first 0.2 ns. (*D*) Fluorescence emission maximum as a function of time for mPlum, mRaspberry, and mRFP in pH 7 buffer as obtained from TCSPC. The excitation wavelength for these measurements was 545 nm.

at 140 K (data not shown). The temperature effect on the dynamic Stokes shift is shown in Fig. 4*B* and was obtained by TCSPC at 298, 270, 230, and 140 K. At 298, 270, and 230 K, the dynamic Stokes shift is characterized by a fast component that is largely complete by 200 ps. Below the glass transition, at 140 K, no dynamic Stokes shift is observed.

Discussion

Solvation Response in mPlum. mPlum is the final product of a long series of mutagenesis steps starting with the tetramer, DsRed, proceeding through monomeric mRFP, and finally via somatic hypermutation to its final red-emitting form. Approximately 5 nm of the shift to redder emission can be attributed to a mutation that is incorporated into the chromophore itself: The Gln-Tyr-Gly sequence that forms the chromophore in DsRed was changed to Met-Tyr-Gly in mRFP (27). The remaining shift results from mutations to residues around the chromophore. mPlum exhibits a substantial dynamic Stokes shift, possible only if the region of the protein solvating the chromophore is capable of some flexibility, yet the mPlum fluorescence quantum yield is reasonably high, suggesting that the directed evolution process has selected for a compromise between flexibility and local rigidity. We consider other possible processes in this *Discussion*.

Solvent reorganization can be monitored by examining the spectral and kinetic components of the fluorescence decay. As shown in Fig. 3*A*, a fast decay component is observed at wavelengths toward the red end of the steady-state emission maximum, and a negative amplitude exponential is required to

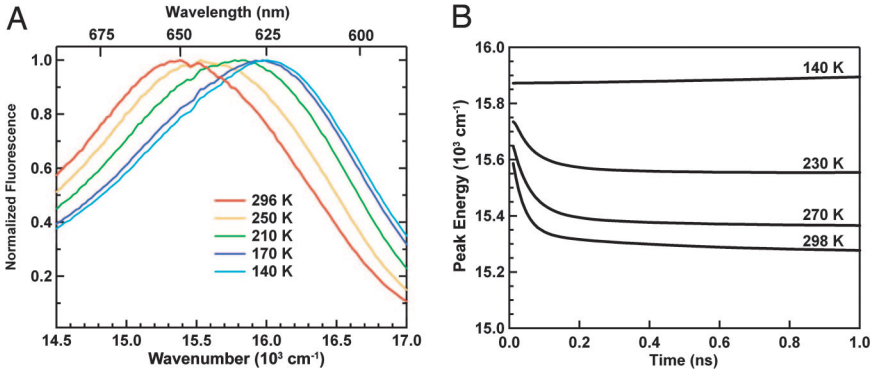

Fig. 4. Temperature dependents. (*A*) Normalized steady-state fluorescence for mPlum at pH 7 from 298 K (red) to 140 K (blue). The excitation wavelength was 466 nm in all cases. (*B*) Fluorescence emission maximum as a function of time for mPlum at pH 7 for temperatures of 298, 270, 230, and 140 K as obtained by TCSPC.

accurately fit the data. This rise in fluorescence amplitude on the red side of the band is characteristic of solvent reorganization as the (protein) environment reorganizes to better solvate the dipolar chromophore excited state. The kinetics are not consistent with two noninterconverting species (or species that interconvert slowly compared with the excited-state lifetime) of different fluorescence lifetimes because only a population transfer, not a difference in lifetime, can produce a rise. Two or more species that interconvert on the timescale of the excited-state lifetime could potentially produce the observed kinetics. However, other data argue against this possibility. The shape of the emission spectra (Fig. 2) and the steady-state anisotropy (data not shown) are the same, irrespective of excitation wavelength. If there were multiple species, it would be likely that each could be preferentially excited at different wavelengths, leading to measurable differences in fluorescence line shape and/or anisotropy. The steady-state anisotropy is high (>0.35) and independent of wavelength; thus, there also is no evidence of a major reorientation or reaction of the chromophore to a photoactive state upon excitation. The time-resolved anisotropy obtained from TCSPC that decays with a single exponential lifetime of ≈14 ns (data not shown) is consistent with the overall rotational correlation time of the protein of 16 ns, which was previously reported for WT GFP and S65T GFP (28), and discounts faster rotation of the entire chromophore with respect to the molecular frame of the protein.

The nature of the fluorescence shift is made clearer by the time-resolved spectra in Fig. 3*B*. The data are consistent with a chromophore excited state that progresses to lower energy as it becomes better solvated. Although the shape of the emission spectrum is largely unchanged as it shifts in energy over time, the FWHM [$\Gamma(t)$ in Eq. **7** of *SI Text*] at pH 7 becomes narrower [from 2,350 cm^{-1} at 10 ps to its final value of ≈2,000 cm^{-1} after 500 ps; before 10 ps, the lack of data points on the high energy side of the band leads to poorly defined $\Gamma(t)$ and inconsistent results between data sets]. Some narrowing on a similar time scale and magnitude also has been observed for a dye in simple solvent (2). This narrowing has been interpreted as an environment that is becoming more organized and ordered over time, leading to slightly less inhomogeneous broadening (2). Apparently, a similar process is possible in the interior of a protein.

The dynamic Stokes shift of mPlum at pH 7 occurs on a timescale of tens of picoseconds, with no evidence for further solvation on the nanosecond time scale. Fitting the peak energy as a function of time with two exponentials (4.3 ps and 71 ps) (Fig. 3*C*) yields results that are slower than observed for dyes in simple, fluid, protic solvents (2) and closer to that observed for tryptophan residues on the surface of a protein (10, 29). The fastest component is likely part of the initial response observed for dyes in protic solvents (30), a fast reorganization and rotation of the relatively unrestrained solvent and side chains around the chromophore. The magnitude of the initial response is likely underestimated given the time resolution of the experiment (instrument response of 400 fs). The solvation response lacks the very slow components (hundreds of picoseconds to nanoseconds) reported for some probes buried or partly buried in proteins, such as dye–protein complexes (5, 7, 31) and unnatural fluorescent amino acids inserted site-specifically at several locations in the sequence of the small protein GB1 (12). However, direct comparison is difficult because, unlike these other systems, mPlum has an intrinsic chromophore that is part of the backbone and protected deep within the protein's β-barrel. Therefore, motions that may be possible within a binding pocket or small protein may be inhibited in mPlum at neutral pH. In contrast, mPlum in pH 11 buffer shows a slow and fast component. The slow component has a lifetime of ≈900 ps compared with the fast components of 3 and 50 ps. The slower component at high pH could be caused by the chromophore environment becoming less rigid as the pH increases. Interestingly, this added flexibility does not come with a major loss in fluorescence because the quantum yield at pH 11 is only slightly lower than at pH 7.

The solvent response in mPlum that produces its far-red emission is not observed in mRFP, its evolutionary ancestor (Fig. 3*D*). The changes in dipole moment between the ground and excited state of mRFP and mPlum were determined to be 6 ± 1 and 5 ± 1 debye, respectively, by electronic Stark spectroscopy (data not shown), similar to GFP (18). Therefore, from the perspective of the electrostatic perturbation associated with excitation, these proteins should be comparable, and the difference in Stokes shift is likely due to the difference in protein solvent.

Temperature Dependence. A blue shift in steady-state fluorescence spectra with decreasing temperature has been attributed to solvation in both small, fluorescent dyes in simple solvents and fluorescent probes in proteins. For dyes in simple solvents, when the temperature is decreased, solvation is slowed due to an increase in viscosity. When the rate of solvation approaches the inverse of the lifetime of the dye, there is a significant contribution to the steady-state spectrum from higher-energy, partially solvated configurations leading to a blue shift in the steady-state spectra at low temperatures. In the few studies of fluorescent probes located in the protein interior, the steady-state spectra also have been shown to shift to higher energy at lower temperatures (5, 32); however, in contrast to simple solvents, studies on a dye–apomyglobin complex showed that, within the studied temperature range of 243–298 K, the rate and magnitude of the solvation response was largely independent of temperature (5). Instead, it was the initial and final emission energies that appear to change with temperature.

As the temperature is lowered, the mPlum steady-state fluorescence emission maximum shifts to higher energy (Fig. 4*A*). This observation can be explained by one of two models. The initial and long-time emission energy may be temperature-dependent. In this case, the protein structure would change with temperature, and we would observe the solvation response between different protein conformations at different temperatures. Alternatively, the initial emission energy may be temperature-independent, but the magnitude of the fast dielectric response that occurs on the timescale of our instrument response may be temperature-dependent. In this case, we may not observe the very fast solvation component, and it would appear as if the solvation response originated from a lower energy state. The time-zero and long-time emission energies increase with decreasing temperature (Fig. 4*B*). However, the rate of the observed solvent reorganization is largely temperature-independent, and a fast solvation component is observed for all temperatures above the glass transition. At 140 K, below the glass transition, no time-dependent Stokes shift is observed. The final emission energies can be confidently determined as all solvation occurring in the first few hundreds of picoseconds, well within the 12-ns measurement window. The lack of appreciable change in the rate of solvation is consistent with a buried chromophore that is largely isolated from the large change in bulk solvent viscosity. The change in steady-state emission spectra can be understood as a change in the final emitting state that is the result of either a temperature-dependent protein structure or a temperature-dependent magnitude of the initial solvation response.

Structural Correlation. Because mPlum was created through a combination of design and *in situ* evolution and we have several of its ancestors in hand, this system offers a unique opportunity to dissect the contributions to spectral shifts and the dynamic Stokes shift. mRaspberry is particularly useful because it

emerged during the evolution from mRFP to mPlum. Because mRaspberry lacks a time-dependent Stokes shift (Fig. 3*D*), the solvation response must be a consequence of mutations that occurred after its development. The mutations that differentiate mRaspberry and mPlum are V16E, R17H, K45R, C65I, G71A, L124V, and K166R. The mutation L124V is associated with a narrowing of the high-energy side of the emission peak but does not change the peak wavelength. Most of these mutations were introduced late in the directed evolution and lead to moderate changes in the extinction coefficient, with little effect on the peak emission maximum that is most indicative of the solvent response. Two mutations however are essential to the far-red emission of mPlum, V16E, and C65I. Saturation mutagenesis showed that variation at either site to any other amino acid led to significant blue-shifted emission or loss of fluorescence (see figure 4 in ref. 24). Therefore, these residues are the focus of discussion.

Residue 65 directly precedes the heterocyclic ring of the chromophore, and the oxidation of its peptide bond extends the chromophore, producing the characteristic red emission of DsRed-derived variants such as mPlum (Fig. 1*D*). The sidechain of E16 is positioned nearby and forms a 2.6-Å-long hydrogen bond with the backbone carbonyl of residue 65, which is part of the extended chromophore. The side chain of residue 65 points away from the chromophore (Fig. 1*D*). The size and shape of the side chain is crucial because mutation to another hydrophobic residue, such as leucine or alanine, leads to a blue shift of the emission by 25 nm. Mutation back to a cysteine, found at residue 65 in mRasberry, leads to a similar blue shift. Because the side chain is hydrophobic and has no direct contact with the chromophore, its contribution to the red emission of mPlum is likely due to packing, which affects the specific interactions of the chromophore within the β-barrel, probably with residue 16.

The hydrogen bond between E16 and the chromophore is believed to be the major cause of mPlum's far-red emission. Removal of this hydrogen bond by mutation to glutamine did not change the position of the sidechain, as confirmed by crystallography (26), but led to a 19-nm shift of emission maximum to the blue. Mutations to other amino acids, such as leucine and histidine, lead to even larger shifts of 30 nm. The solvation response in mPlum can then be explained as a time-dependent interaction between E16 and the excited state of the chromophore. The simplest explanation for the time dependence is a rotation of the glutamic acid in response to the new charge distribution of the excited state.

The link between E16 and the red shift suggests that the dynamic Stokes shift is the result of a specific excited-state rearrangement between the chromophore and a strongly interacting sidechain. This interpretation differs from canonical solvation theory, where a collection of solvent dipoles stochastically rearranges around the excited-state dipole of a chromophore. However, the possibility that the mutation causes other changes or increases the general flexibility of the chromophore environment, including water inside the β-barrel, cannot be dismissed. Flexibility of the chromophore environment would be expected to lead to a lower quantum yield. It is unclear whether increased flexibility around the chromophore is the cause of the lower quantum yield for mPlum compared with mRFP and mRaspberry.

Materials and Methods

Protein Expression and Purification. A pBAD (Invitrogen) plasmid construct containing the mPlum gene (24) was generously supplied by Roger Tsien (University of California at San Diego, La Jolla, CA). Protein expression was performed as recommended by Invitrogen for the pBAD expression system. After expression, the cells were lysed in a homogenizer (Avestin) and chromophore-containing proteins were isolated with a Ni-NTA column. The post-translational modifications that form the mature mPlum chromophore do not always proceed to completion. The modifications involve cyclization and two oxidation reactions, the first of which forms a GFP-like chromophore (immature chromophore), which is then extended by the second oxidation to form a DsRed-like chromophore (33). Chemical structures of the mature and immature chromophores are shown in Fig. 1. The immature mPlum chromophore is a dead-end side product and has very weak green fluorescence. Because immature and mature mPlum chromophores absorptions are well separated (λ_{max} = 502 and 580 nm, respectively), it is straightforward to determine the amounts of each (typically 50% of each under our growth conditions), but separation of the two proteins, differing only in the pK_a of the chromophore, is difficult. (Note that GFP absorption spectra in the literature often are fluorescence excitation spectra that select for the mature form and hide the nonfluorescent immature form, even when a substantial amount is present.)

Separation of immature and mature mPlum was achieved by anion exchange chromatography: a P900 (Amersham Biosciences) FPLC provided a constant flow rate of 2.00 ml/min through four 5-ml HiTrap SP HP columns (Amersham Biosciences) connected in tandem. Elution occurred with a pH gradient in 50 mM citrate buffer from pH 5 to pH 6 over 150 ml. After elution, protein was exchanged into pH 7, 50 mM Mops, 100 mM NaCl buffer and stored at 4°C. mRFP (10) and mRaspberry (24) were grown and purified by the same procedure. The mRFP1.2 variant (27) was used exclusively in this study and is referred to as mRFP for simplicity.

Absorption and Steady-State Fluorescence Spectroscopy. Absorption and steady-state fluorescence spectra were obtained with a Cary 6000i (Varian) and a FluoroLog-3 (Horiba Jobin Yvon) spectrometer, respectively. Variable temperature measurements from 298 to 140 K were performed on mPlum in 60/40 glycerol/buffer solution using a miniature Joule–Thomson refrigerator (MMR Technologies) and a 1-mm sample geometry, with temperature calibration as described in detail elsewhere (8). Electronic Stark spectra were obtained and analyzed as previously described (34).

Time-Resolved Emission Spectroscopy. With the exception of the excitation source described below, fluorescence upconversion spectroscopy (34, 35) and TCSPC (36) were performed largely as described previously. Excitation light at 580 nm (or 540 nm for some experiments) was obtained from the pulsed, supercontinuum output from a photonic crystal fiber (Femtowhite). Upconversion with photonic crystal fiber excitation produced a Gaussian instrument response function of ≈400 fs at FWHM, for TCSPC it is a series of Gaussians of ≈30 ps at FWHM. The photonic crystal fiber was pumped with 800 nm light at 82 MHz with a Ti:Sapphire oscillator (average pump power of the 100-fs pulses was 400 mW). A Faraday isolator (OFR, Inc.) was inserted before the photonic crystal fiber because back reflection from the fiber was sufficient to interrupt the mode locking of the laser. A half waveplate (Newport) was used to control the polarization of the input beam, and a ×60 microscope lens (Thorlabs) was used to couple the light to the fiber. The fiber generated a continuum of light from ≈500 to 700 nm, and a 20-nm band pass filter centered at 580 nm (Chroma Technology) was used to select the appropriate light for mPlum excitation with an average excitation power between 2 and 3 mW. For some experiments, excitation light centered at 540 nm with a 10-nm bandpass was used. Collimation after the photonic crystal fiber was achieved with a ×60 microscope lens identical to the input lens, and a broadband half waveplate (Newport) was used to control excitation polarization.

ACKNOWLEDGMENTS. We thank Profs. Roger Tsien and Lei Wang (now at the Salk Institute, La Jolla, CA) for providing the clone for mPlum and for many useful discussions; Prof. S. James Remington and Dr. Xiaokun Shu (both at University of Oregon, Eugene, OR) for crystallizing mature and immature mPlum and providing the coordinates for the chromophore and nearby amino acids (Fig. 1); Timothy B. McAnaney for helpful discussion; and Tony Kanchanawong for the determination of the change in dipole moment for mRFP and mPlum by electronic Stark spectra. This work was supported in part by National Institutes of Health Grant GM27738 (to S.G.B.). The fluorescence upconversion facilities were supported by the Medical Free Electron Laser Program of the Air Force Office of Scientific Research through Grant F49620-00-1-0349. X.S. was supported by a William R. and Sara Hart Kimball Stanford Graduate Fellowship. P.A. was supported by the Fonds de Recherche sur la Nature et les Technologies and the National Science and Engineering Research Council of Canada.

1. Van der Zwan G (1985) *J Phys Chem* 89:4181–4188.
2. Horng ML, Gardecki JA, Papazyan A, Maroncelli M (1995) *J Phys Chem* 99:17311–17337.
3. Matz MV, Fradkov AF, Labas YA, Savitsky AP, Zaraisky AG, Markelov ML, Lukyanov SA (1999) *Nat Biotech* 17:969–973.
4. Homoelle BJ, Edington MD, Diffey WM, Beck WF (1998) *J Phys Chem B* 102:3044–3052.

5. Pierce D, Boxer SG (1992) *J Phys Chem* 96:5560–5566.
6. Sahu K, Mondal SK, Ghosh S, Roy D, Bhattacharyya K (2006) *J Chem Phys* 124:124909.
7. Bashkin JS (1990) *J Phys Chem* 94:4757–4761.
8. Zimmermann J, Oakman EL, Thorpe IF, Shi X, Abbyad P, Brooks CL, III, Boxer SG, Romesberg FE (2006) *Proc Natl Acad Sci USA* 103:13722–13727.
9. Bhattacharyya SM, Wang ZG, Zewail AH (2003) *J Phys Chem B* 107:13218–13228.
10. Campbell RE, Tour O, Palmer AE, Steinbach PA, Baird GS, Zacharias DA, Tsien RY (2002) *Proc Natl Acad Sci USA* 99:7877–7882.
11. Lu WY, Kim J, Qiu WH, Zhong DP (2004) *Chem Phys Lett* 388:120–126.
12. Cohen BE, McAnaney TB, Park SE, Jan YN, Boxer SG, Jan LY (2002) *Science* 296:1700–1703.
13. Abbyad P, Shi X, Childs W, McAnaney TB, Cohen BE, Boxer SG (2007) *J Phys Chem B* 111:8269–8276.
14. Lampa-Pastirk S, Lafuente RC, Beck WF (2004) *J Phys Chem B* 108:12602–12607.
15. Lampa-Pastirk S, Beck WF (2004) *J Phys Chem B* 108:16288–16294.
16. Owens TG, Webb SP, Alberte RS, Mets L, Fleming GR (1988) *Biophys J* 53:733–745.
17. Ormö, M., Cubitt AB, Kallio K, Gross LA, Tsien RY, Remington SJ (1996) *Science* 273:1392–1395.
18. Bublitz G, King BA, Boxer SG (1998) *J Am Chem Soc* 120:9370–9371.
19. Dong J, Solntsev KM, Tolbert LM (2006) *J Am Chem Soc* 128:12038–12039.
20. Webber NM, Litvinenko KL, Meech SR (2001) *J Phys Chem B* 105:8036–8039.
21. Ward WW, Bokman SH (1982) *Biochemistry* 21:4535–4540.
22. Sharafy S, Muszkat KA (1971) *J Am Chem Soc* 93:4119–4125.
23. Mauring K, Deich J, Rosell FI, McAnaney TB, Moerner WE, Boxer SG (2005) *J Phys Chem B* 109:12976–12981.
24. Wang L, Jackson WC, Steinbach PA, Tsien RY (2004) *Proc Natl Acad Sci USA* 101:16745–16749.
25. Shaner NC, Steinbach PA, Tsien RY (2005) *Nat Methods* 2:905–909.
26. Shu X, Shaner NC, Yarbrough CA, Tsien RY, Remington SJ (2006) *Biochemistry* 45:9639–9647.
27. Shaner NC, Campbell RE, Steinbach PA, Giepmans BNG, Palmer AE, Tsien RY (2004) *Nat Biotech* 22:1567–1572.
28. Volkmer A, Subramaniam V, Birch DJS, Jovin TM (2000) *Biophys J* 78:1589–1598.
29. Peon J, Pal SK, Zewail AH (2002) *Proc Natl Acad Sci USA* 99:10964–10969.
30. Jimenez R, Fleming GR, Kumar PV, Maroncelli M (1994) *Nature* 369:471–473.
31. Jordanides XJ, Lang MJ, Song XY, Fleming GR (1999) *J Phys Chem B* 103:7995–8005.
32. Vincent M, Gilles AM, Li de laSierra IM, Briozzo P, Barzu O, Gallay J (2000) *J Phys Chem B* 104:11286–11295.
33. Gross LA, Baird GS, Hoffman RC, Baldridge KK, Tsien RY (2000) *Proc Natl Acad Sci USA* 97:11990–11995.
34. Chattoraj M, King BA, Bublitz GU, Boxer SG (1996) *Proc Natl Acad Sci USA* 93:8362–8367.
35. Stanley RJ, Boxer SG (1995) *J Phys Chem* 99:859–863.
36. McAnaney TB, Zeng W, Doe CFE, Bhanji N, Wakelin S, Pearson DS, Abbyad P, Shi X, Boxer SG, Bagshaw CR (2005) *Biochemistry* 44:5510–5524.